DE-FG05-80ET-53088-666 IFSR #666

Ion Orbit Loss and the Poloidal Electric Field in a Tokamak

H. XIAO, R.D. HAZELTINE
Institute for Fusion Studies
The University of Texas at Austin
Austin, Texas 78712
and
P.M. VALANJU
Fusion Research Center
The University of Texas at Austin
Austin, Texas 78712

July 1994

July 29, 1994

Ion orbit loss and the poloidal electric field in a tokamak

H. Xiao, R. D. Hazeltine

Institute for Fusion Studies, The University of Texas at Austin

Austin, Texas 78712

and

P. M. Valanju

Fusion Research Center, The University of Texas at Austin, Austin, Texas 78712

Abstract

Monte-Carlo simulation studies for ion orbit loss in limiter tokamaks show a poloidal asymmetry in ion loss arising from differences in ion orbit geometry. Since electron loss to the limiter is uniformly distributed because of its tiny orbit width, the nonuniform ion loss could cause a poloidal electric field that would tend to make the ion loss to the limiter more uniform. A simple analytical derivation of this poloidal electric field and a discussion of its effects on ion movement and transport are also presented.

I. INTRODUCTION

Poloidal asymmetry of electric potential has been observed in many tokamaks,[1-6] and there are several theoretical works discussing the origin of the poloidal electric field. It was found that the poloidal electric field could be produced by neutral beam injection, which leads to many trapped ions in the outer side (low field side) of the torus.[7] High power ion cyclotron resonance heating (ICRH) and electron cyclotron resonance heating (ECRH) also could cause in-out poloidal asymmetry for a similar reason. Even in an ohmically-heated tokamak a steady-state poloidal electric field is possible, due to a high concentration of impurity particles,[8,9] or high-collisional friction in the edge plasma.[10]

Hazeltine and Ware,[8] Chang,[11] and Indireshkumar and Stacey[12] have investigated the effects of poloidal electric field of order ϵ on plasma transport, where $\epsilon = r/R$ is the inverse aspect ratio. They found that the plasma transport could be enhanced by a factor of two due to the convective flux caused by the $\mathbf{E} \times \mathbf{B}$ drift.

It is well known that the ion orbit plays a very important role in forming the radial electric field near the plasma edge,[13,14] and recently its effect on the poloidal electric field has also been studied.[6,15] Because the electron orbit width is very small, the orbit effect on the electron loss to the tokamak limiter should be negligible. Thus we can assume that the electron loss is uniformly distributed in the poloidal direction. However, the ion loss to the limiter

or divertor is dominated by orbit effects and strongly varies in the poloidal direction. A poloidal electric field is formed by the unequally distributed electrons and ions near the tokamak plasma edge, and this field reduces the nonuniformity of the ion orbit loss. This poloidal electric field only exists near the edge, i.e., within about one banana width of the last closed flux surface (LCFS).

In Sec. II we give a simple analytical derivation of the poloidal electric field induced by ion orbit loss. Monte-Carlo simulation studies of effects of E_θ and E_r on particle orbits and transport are given in Sec. III. In Sec. IV, we give a brief discussion and summary.

II. DERIVATION OF POLOIDAL ELECTRIC FIELD

The steady-state ion continuity equation with ion orbit loss can be presented as

$$\nabla \cdot (n\mathbf{V}) = \nu\gamma(\theta)n \ , \tag{1}$$

where n is the ion density, ν is the ion collision frequency and $\gamma(\theta)$ is the poloidal ion loss pattern to the limiter, $0 < \gamma < 1$. Assume that the perpendicular ion flow velocity $\mathbf{V}$ is dominated by the $\mathbf{E} \times \mathbf{B}$ drift, and that the parallel flow has been slowed down by the neutral particles via charge exchange. Then the continuity equation can be written as

$$\nabla \cdot \left(\frac{n}{B^2} \mathbf{E} \times \mathbf{B} \right) = \nu\gamma(\theta)n \ . \tag{2}$$

Using a magnetic field in toroidal coordinates

$$\mathbf{B} = I\nabla\zeta + \nabla\zeta \times \nabla\chi \,, \tag{3}$$

Maxwell's equation

$$\nabla \times \mathbf{B} = \frac{4\pi}{c}\mathbf{J} \,, \tag{4}$$

and

$$\mathbf{E} = -\nabla\phi \,, \tag{5}$$

where ζ is the toroidal flux, χ is the poloidal flux, and $I = RB_0$, we can obtain the equation

$$\frac{IB_p}{\chi'}\left[\overline{\phi}_r\left(\frac{cn}{B^2}\right)_\theta - \widetilde{\phi}_\theta\left(\frac{cn}{B^2}\right)_r\right] + \frac{4\pi n}{B^2}\left(\overline{\phi}_r J^r + \widetilde{\phi}_\theta J^\theta\right) = \nu\gamma(\theta)n \,. \tag{6}$$

Here subscripts indicate derivatives with respect to the variables, superscripts indicate the corresponding components, overbars represent the average over θ, and tildes represent the variation over θ. Assume the r-derivative is of order $\mathcal{O}(1)$ and the θ-derivative is of order $\mathcal{O}(\epsilon)$. Noting that $\widetilde{n}$ is also of order $\mathcal{O}(\epsilon)$, to first order in ϵ, we have

$$\frac{cIB_p}{\chi' B_0^2}\left[\overline{\phi}_r\widetilde{n}_\theta - \widetilde{\phi}_\theta\overline{n}_r\right] + \frac{4\pi}{B_0^2}\left(\widetilde{n}\overline{\phi}_r J^r + \overline{n}\widetilde{\phi}_\theta J^\theta\right) = \nu\gamma(\theta)\overline{n} \,. \tag{7}$$

From quasineutrality and assuming that the electron density obeys the Boltzmann distribution, $n_e = n_0 e^{e\phi/T}$, we get

$$\overline{n} \approx n_0 \exp\left(\frac{e\overline{\phi}}{T}\right) \,, \tag{8}$$

and

$$\tilde{n} \approx n_0 \frac{e\tilde{\phi}}{T} \exp\left(\frac{e\overline{\phi}}{T}\right) . \tag{9}$$

Assuming radial current $J^r = 0$, we obtain:

$$\tilde{\phi}_\theta = \nu\gamma(\theta) \Big/ \left\{ \frac{cIB_p}{\chi' B_0^2} \left[\frac{e\overline{\phi}_r}{T} - (\ln \overline{n})_r \right] + \frac{4\pi}{B_0^2} J^\theta \right\} . \tag{10}$$

This result seems reasonable because the dependence of electrical potential ϕ on the poloidal angle θ is weak, and it is caused by the nonsymmetric ion loss as expected.

It is very difficult to calculate the self-consistent ion loss pattern $\gamma(\theta)$ analytically, but it is not very hard to obtain by Monte-Carlo simulation.[16] We get the radial electric field caused by the nonuniform ion orbit loss by substituting the ion loss pattern obtained from simulation into Eq. 10. Then we substitute the poloidal electric field into the Monte-Carlo simulation code to get the ion orbit loss pattern $\gamma(\theta)$. We close the self-consistent loop when both poloidal electric field and ion loss pattern approximately satisfy Eq. 10.

III. PARTICLE ORBITS AND MONTE-CARLO SIMULATION RESULTS

The typical ion banana orbit in a counterclockwise (top view) toroidal field, positive helicity torus (plasma current parallel to the toroidal magnetic field) is shown in Fig. 1. The ion orbit is determined by the direction of ion drift, which is upward in this case. From Fig. 1 we find that the trapped

ion always drifts upward in the inner part of the orbit and downward in the outer part of the orbit. Thus the ion banana orbits always tend to reach the limiter from the outside (low field side) and upper half of the torus. We can get the ion orbit loss patterns on a ring limiter by the Monte Carlo simulation. The results in the banana regime ($\nu/(v_t/R) = 0.005$) and the plateau regime ($\nu/(v_t/R) = 0.05$) without poloidal electric field are shown in Figs. 2 and 3, respectively. As expected, the ion orbit losses to the limiter are concentrated in the outside and upper half of the torus in the banana regime, and concentrated in the upper half of the torus in the plateau regime, because collisions weakened the banana orbit effects. In both cases, the ion loss patterns are clearly nonsymmetric in the poloidal direction. Thus poloidal electric fields caused by nonsymmetric ion loss can be expected, and in return, will reduce the asymmetry in the ion loss pattern.

The simulation result of ion loss pattern with Lorentz form of radial electrostatic potential in the plateau regime is shown in Fig. 4.

$$\phi(r) = \frac{\phi_1}{1 + \left(\frac{r - r_s}{\Delta r}\right)^2} .$$

We find that the ion loss pattern is almost the same as that from a constant radial electric field. Therefore, in this work we choose the constant radial electric field so that we can focus our attention on the relation between the poloidal electric field and the ion loss pattern.

Since a higher electric potential will develop in the upper half to prevent

ion loss concentration there, we choose the poloidal electric potential as

$$\widetilde{\phi} = \phi_0 \sin\theta \ .$$

The ion orbit in this electric field is shown in Fig. 5. We find that the ion orbit is pushed to the lower part of the torus, and the orbit width is increased. This kind of electric potential could help increase the ion orbit loss in the lower half and balance the ion loss in the upper half of the torus.

The Monte-Carlo simulation results in banana regime and plateau regime with this electric potential are given in Figs. 6 and 7, respectively. We find that the total ion orbit loss is increased and the loss pattern is better balanced in the upper and lower part, as compared to the case without the poloidal electric field. From Eq. 10, we know that the poloidal electric field is proportional to the ion loss pattern, so that the $\cos\theta$-like loss pattern ($\gamma(\theta) \approx \cos\theta$) shown in Figs. 6 and 7 should yield a $\cos\theta$-like poloidal electric field, or $\sin\theta$-like electric potential. This is consistent with experimental observations in Alcator-C[17,1] and Texas Experimental Tokamak Upgrade (TEXT-U).[18,19]

IV. DISCUSSION AND SUMMARY

From the approximately self-consistent relation between ion loss patterns and Eq. 10, we found the ion loss pattern $\gamma(\theta) \approx \cos\theta$ in both the banana and plateau regimes. Comparing the three terms in the denominator in Eq. 10,

we find

$$\frac{\text{2nd term}}{\text{1st term}} = \frac{a}{n}\frac{\partial n}{\partial r}\Big/\frac{eE_r a}{T} \ll 1 ,$$

and

$$\frac{\text{3rd term}}{\text{1st term}} = \frac{4\pi}{cB}J^{\theta}\Big/\frac{eE_r}{T} = -\frac{1}{B}\frac{\partial B}{\partial r}\Big/\frac{eE_r}{T} \approx \frac{T}{eE_r R} \ll 1 .$$

Therefore we can simplify Eq. 10 to:

$$\tilde{\phi}_{\theta} \approx \nu\frac{\chi' B_0^2 T}{cIB_p e\phi_r}\cos\theta .$$

Then we can get the relation between electrostatic potential and poloidal angle for the banana and plateau regimes after a simple derivation:

$$\frac{e\tilde{\phi}(\theta)}{T} \approx \frac{a\nu B_0}{cE^r}\sin\theta . \qquad (11)$$

In TEXT-U experiments, the collision frequencies near the edge are mainly in the plateau regime. Using TEXT-U data we get the top-bottom potential difference from Eq. 11:

$$\frac{e\Delta\tilde{\phi}}{T} = e\left[\tilde{\phi}(\pi/2) - \tilde{\phi}(-\pi/2)\right]\Big/T$$

of about 0.1 to 1, in agreement with the experimental measurement of about 0.5.

The difference between the top and bottom potentials quickly drops to zero when density increases and electron temperature decreases.[19] This is because strong collisions almost wiped out the banana orbit effects and made ion loss to the limiter up-down symmetric. Figure 8 shows that strong collision ($\nu/(v_t/R) = 1.5$) can effectively weaken the top-bottom asymmetry of

the ion orbit loss pattern. In this case E_θ will be of the form $\sin\theta$ with no top-bottom potential difference.

Because ion loss pattern is determined by the ion drift orbit, we expect that by changing the direction of the toroidal magnetic field, which changes the direction of $\mathbf{B} \times \nabla B$ drift, the poloidal electric field will change direction. We can use this property to understand the experimental results of Alcator-C and JFT-2M.[20] We can also expect that the electric potential in the bottom will be higher than that in the top if the direction of the magnetic field in TEXT-U is reversed.

A poloidal asymmetry of the impurity distribution near the plasma edge is also observed in TEXT-U.[21] This might further support our model because the ion bombardment of the limiter generates a major component of the impurity source.

Our simulation results show that this poloidal electric field leads to an outward convection flux that can be larger than the neoclassical diffusive flux. Without the poloidal electric field, the neoclassical ion loss rate in both banana and plateau regimes is less than a fourth of its value for the representative case, $\tilde{\phi} = \phi_0 \sin\theta$, $\phi_0 = 0.5 m v_t^2/e$. This agrees with previous theories.[8,11,12]

With a modest negative or a very large positive radial electric field, the ion orbit loss reduces dramatically, due to ion mobility.[22] The poloidal electric field may also reduce along with the total ion orbit loss. As a result, a

transport barrier is formed. The steep density profile near the edge, caused by the transport barrier, can form a shoulder-like kink in the electron density profile that can help maintain the sheared negative electric field that the transport barrier needs.[14] This scenario may help us understand the spontaneous high-confinement mode (H-mode).

In summary, a simple theoretical model of a steady-state poloidal electric field based on asymmetric ion orbit loss in limiter tokamaks has been developed. The results appear to agree well with the experimental measurements in TEXT-U.

Acknowledgment

We acknowledge helpful discussions with R. D. Bengtson, G. X. Li, A. J. Wootton, W. L. Rowan, and E. Solano. This work was supported by the U.S. Department of Energy contract #DE-FG05-80ET-53088.

References

[1]B. Labombard and B. Lipschultz, Nucl. Fusion **27**, 81 (1987).

[2]R. A. Pitts, G. Vayakis, G. F. Matthews, and V. A. Vershkov, J. Nucl. Materials **176-177**, 893 (1990).

[3]A. V. Nedospasov, S. S. Bychkov, V.V. Gaponov, N. M. Zykoza, R. S. Ivanov, V. N. Kabznov, Ju. V. Nekrylova, A. V. Sazonov, and G. I. Stotsky, J. Nucl. Materials **176-177**, 169 (1990).

[4]V. P. Budaev, L. M. Bogomolov, B. V. Borovsky, R. S. Ivanov, E. D. Lazarev, A. V. Nedospasov, A. A. Rakovets, V. N. Sychev, Y. A. Trapeznikov, and A. V. Chernlevsky, J. Nucl. Materials **176-177**, 705 (1990).

[5]G. R. Tynan, L. Schmitz, R. W. Conn, R. Doerner, and R. Lehmer, Phys. Rev. Lett. **68**, 3032 (1992).

[6]H. Ohtsuka, JFT-2 group, Nucl. Fusion **33**, 523 (1993).

[7]C. S. Chang, R.W. Harvey, Nucl. Fusion **23**, 935 (1983).

[8]R. D. Hazeltine and A. A. Ware, Physics of Fluids **19**, 1163 (1976).

[9]C. S. Chang and R. D. Hazeltine, Physics of Fluids **25**, 536 (1982).

[10]C. S. Chang and R. D. Hazeltine, Nucl. Fusion **20**, 1397 (1980).

[11]C. S. Chang, Physics of Fluids **26**, 2140 (1983).

[12]K. Indireshkumar and W. M. Stacey, Jr., Physics of Fluids B **5**, 1850 (1993).

[13]R. D. Hazeltine, Physics of Fluids B **1**, 2031 (1989).

[14]R. D. Hazeltine, H. Xiao, and P. M. Valanju, Physics of Fluids B **5**, 4011 (1993).

[15]M. Tendler, U. Daybelge, and V. Rozhansky, *Plasma Phys. Contr. Nucl. Fusion*, Proc. on 14th Conference, (Würzburg, Germany, 1992) Vol. 2, p. 243.

[16]H. Xiao, R. D. Hazeltine, P. M. Valanju, and Y. Z. Zhang, Bull. Am. Phys. Soc. **38**, 1928 (1993).

[17]I. H. Hutchinson and S. E. Kissel, Physics of Fluids **23**, 1698 (1980).

[18]P. H. Edmonds, E. R. Solano, A. J. Wootton, D. Gao, X. Mao, G. Li, and W. Zhu, "Fusion Technology 1988," (Elsevier Science Pub B.V., 1989), p. 342.

[19]G. X. Li, R. D. Bengtson, H. Lin, M. Meier, H. Y. W. Tsui, and A. J. Wootton, *The Plasma Potential Asymmetry and Steady-State Radial Convection in TEXT-U Tokamak*, submitted to Nucl. Fusion.

[20]H. Tamai, K. Odajima, H. Matsumoto, T. Ogawa, H. Kimura, K. Hoshino, S. Kasai, T. Kawakami, H. Kawashima, M. Maeno, M. Mori, I. Ochiai.

H. Ogaawa, K. Ota, H. Ohtsuka, S. Sengoku, T. Shoji, N. Suzuki, Y. Uesugi, S. Yamamoto, T. Yamamoto, T. Yamauchi, and I. Yanagisawa, Nucl. Fusion **26**, 365 (1986).

[21]R. A. Collin and W. L. Rowan, private communication, 1994.

[22]H. Xiao, R. D. Hazeltine, Y. Z. Zhang, and P. M. Valanju, Physics of Fluids B **5**, 4499 (1993).

Figure Captions

Fig. 1 Ion banana orbit without poloidal electric field. Parameters: $r_0/a = 0.7$, $\theta_0 = 0$, $v_0 = 2.5$, $\xi = 0.1$, $eE_r a/mv_t^2 = 20$, $a/R = 0.3$, $\rho/a = 0.002$, $q_a = 4.0$, and $\nu/(v_t/R) = 0$. Where $\xi = v_{||,0}/v_0$ is the pitch angle, $\rho = eB/mc$ is gyro radius, and q_a is the safety factor on the plasma edge.

Fig. 2 Ion orbit loss pattern in banana regime without poloidal electric field. Parameters: $r_0/a = 0.925$, $eE_r a/mv_t^2 = 20$, $a/R = 0.3$, $\rho/a = 0.002$, $q_a = 4.0$, and $\nu/(v_t/R) = 0.005$.

Fig. 3 Ion orbit loss pattern in plateau regime without poloidal electric field. Parameters: $r_0/a = 0.925$, $eE_r a/mv_t^2 = 20$, $a/R = 0.3$, $\rho/a = 0.002$, $q_a = 4.0$, and $\nu/(v_t/R) = 0.05$.

Fig. 4 Ion orbit loss pattern in plateau regime with Lorentz radial potential without poloidal electric field. Parameters: $r_0/a = 0.925$, $a/R = 0.3$, $\rho/a = 0.002$, $q_a = 4.0$, $\nu/(v_t/R) = 0.05$, $e\phi_1/mv_t^2 = 1$, $\Delta r/a = 0.02$, and $r_s/a = 0.925$.

Fig. 5 Ion banana orbit with poloidal electric field, $\phi(\theta) = \phi_0 \sin\theta$, where $e\phi_0/mv_t^2 = 1$. Other parameters are the same as for Fig. 1.

Fig. 6 Ion orbit loss pattern in banana regime with poloidal electric field, $\phi(\theta) = \phi_0 \sin\theta$, where $e\phi_0/mv_t^2 = 1$. Other parameters are the same as for Fig. 2.

Fig. 7 Ion orbit loss pattern in plateau regime with poloidal electric field, $\phi(\theta) = \phi_0 \sin\theta$, where $e\phi_0/mv_t^2 = 1$. Other parameters are the same as for Fig. 3.

Fig. 8 Ion orbit loss pattern in collisional regime without poloidal electric field. Parameters: $r_0/a = 0.925$, $eE_r a/mv_t^2 = 20$, $a/R = 0.3$, $\rho/a = 0.002$, $q_a = 4.0$, and $\nu/(v_t/R) = 1.5$.

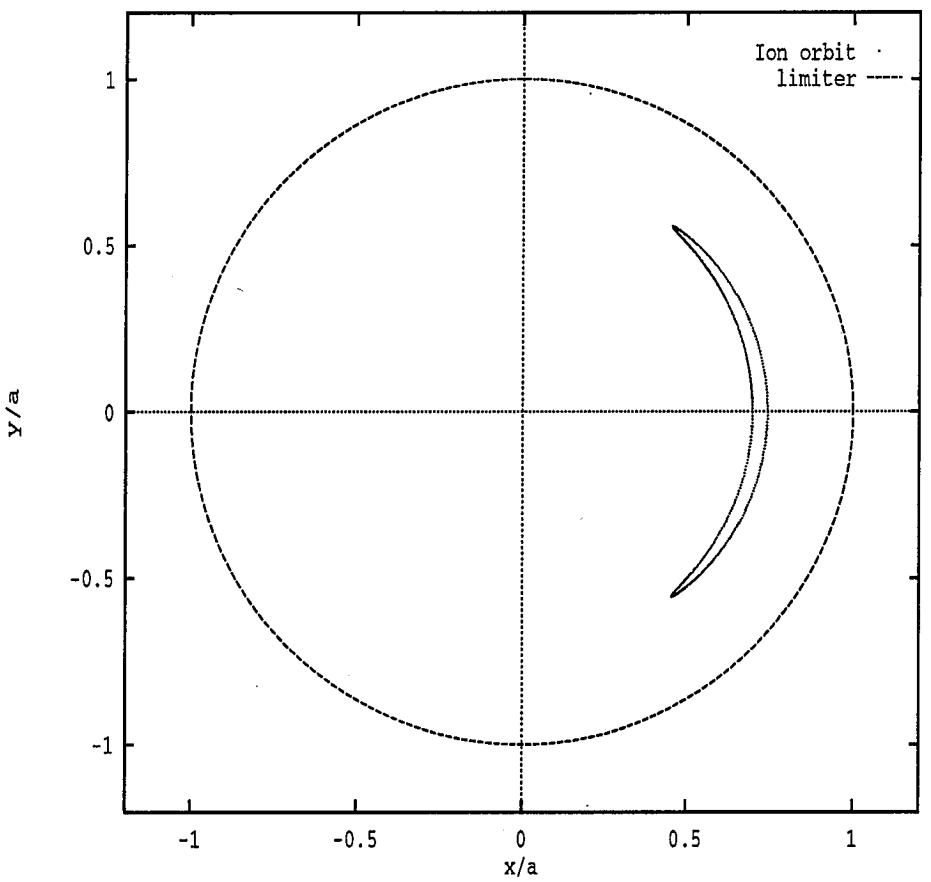

Figure 1: Xiao, PoP-20539

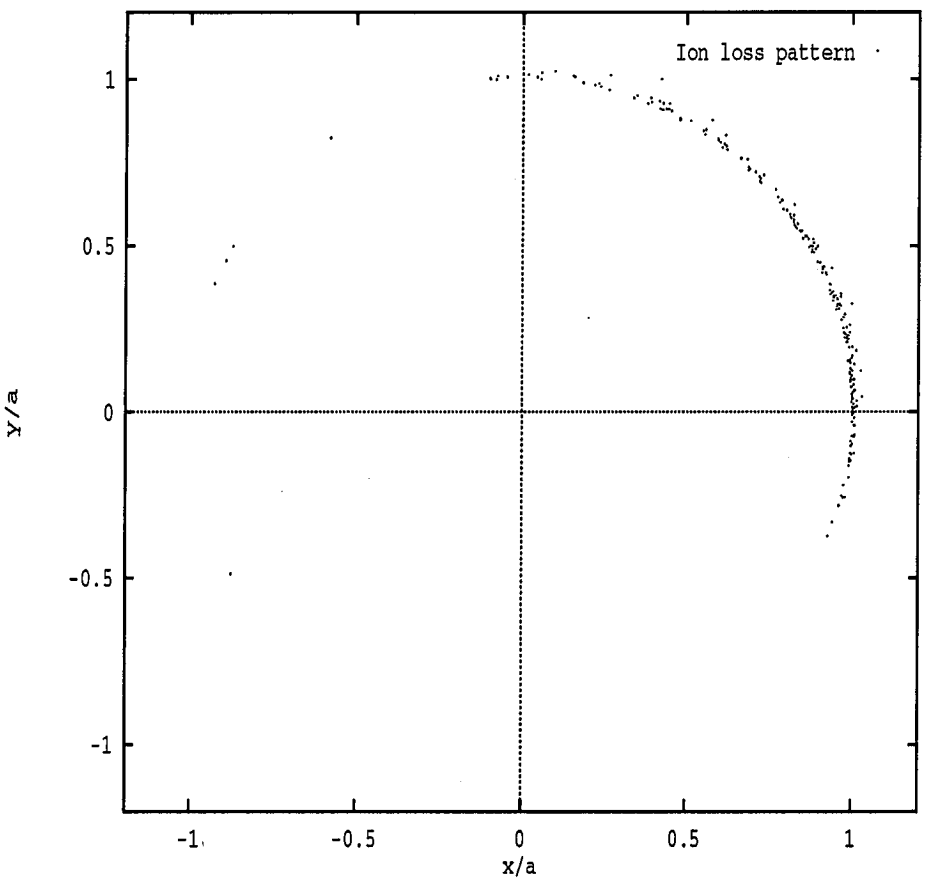

Figure 2: Xiao, PoP-20539

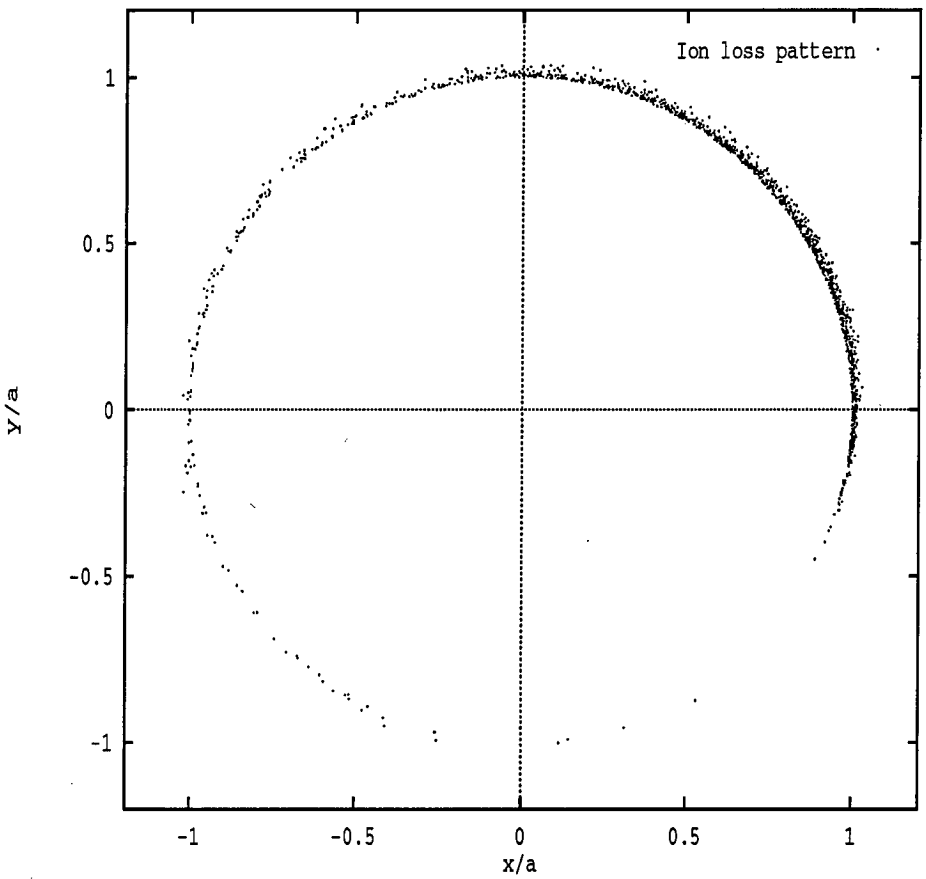

Figure 3: Xiao, PoP-20539

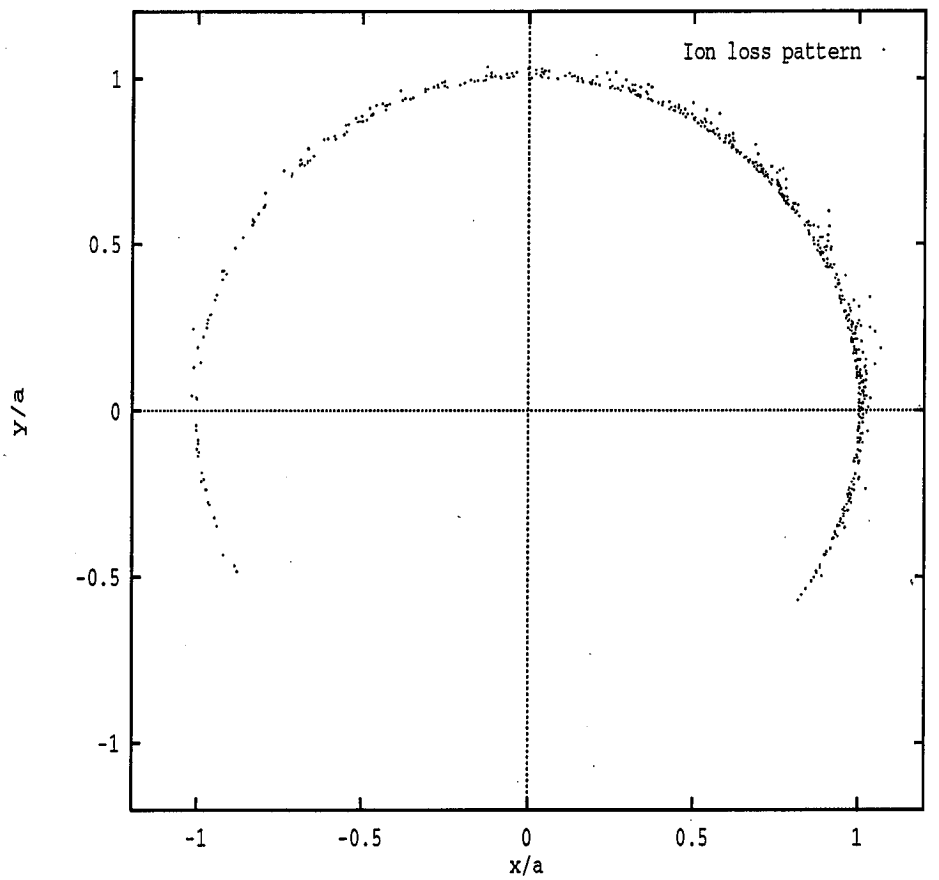

Figure 4: Xiao, PoP-20539

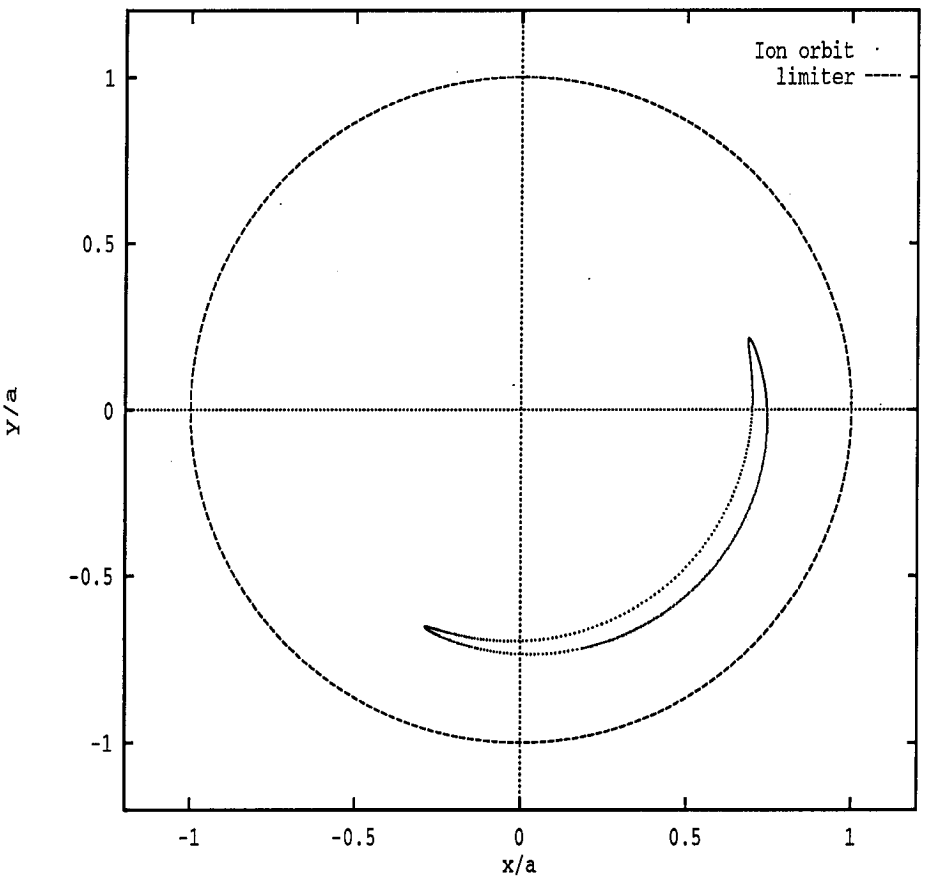

Figure 5: Xiao, PoP-20539

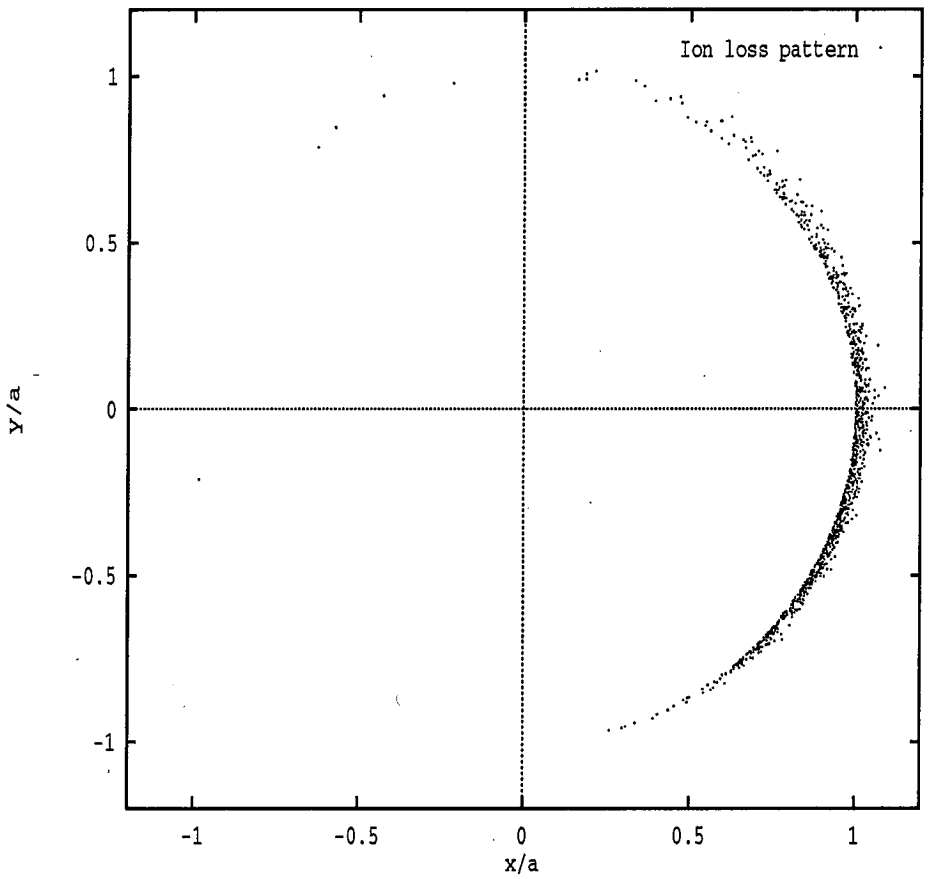

Figure 6: Xiao, PoP-20539

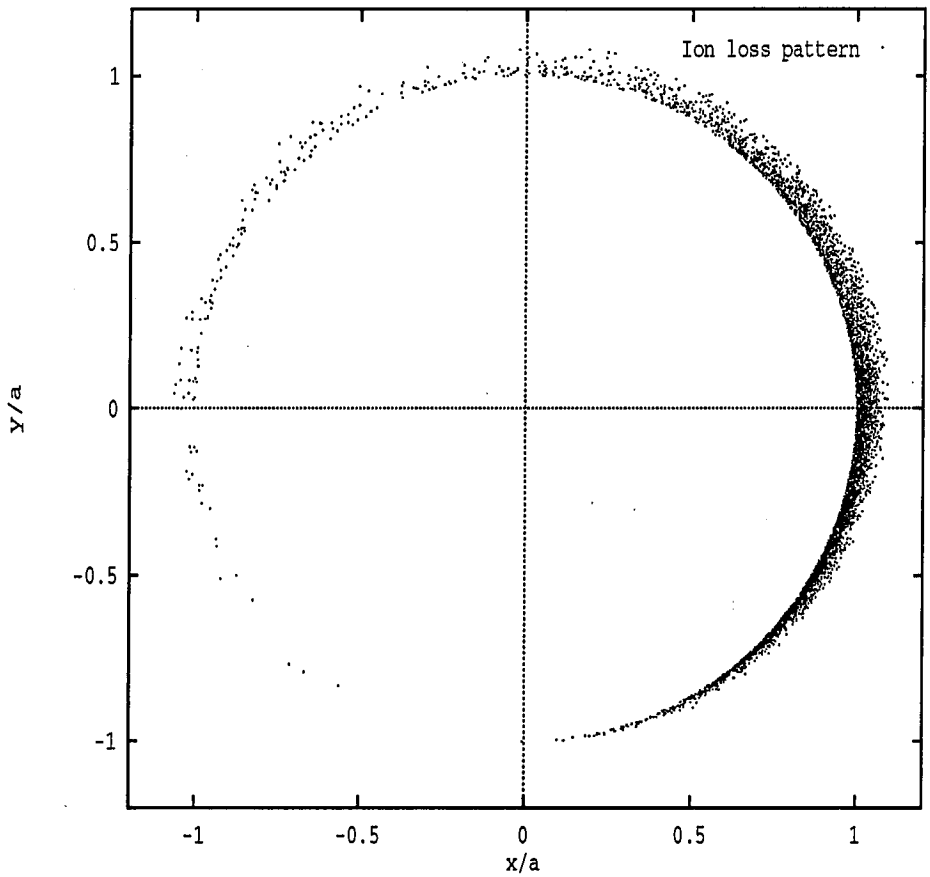

Figure 7: Xiao, PoP-20539

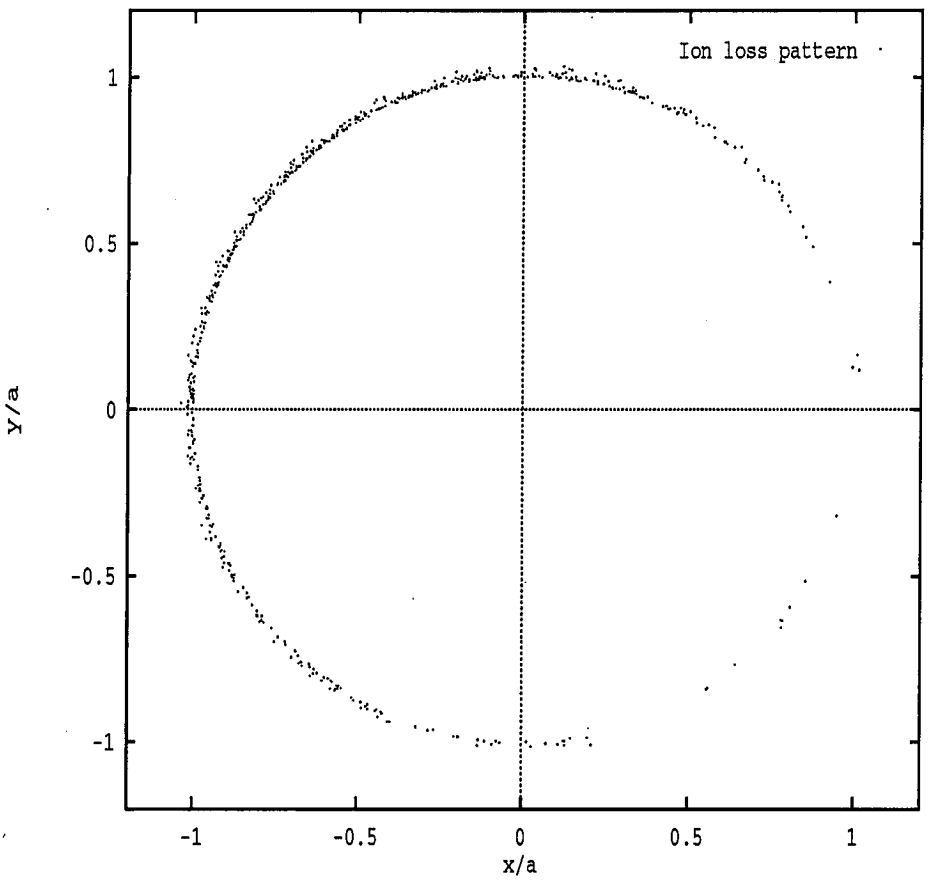

Figure 8: Xiao, PoP-20539